Science & Technology Facilities Council
ISIS

MATERIAL RESPONSE TO HIGH POWER BEAMS

Goran Škoro

ISIS, STFC, UK

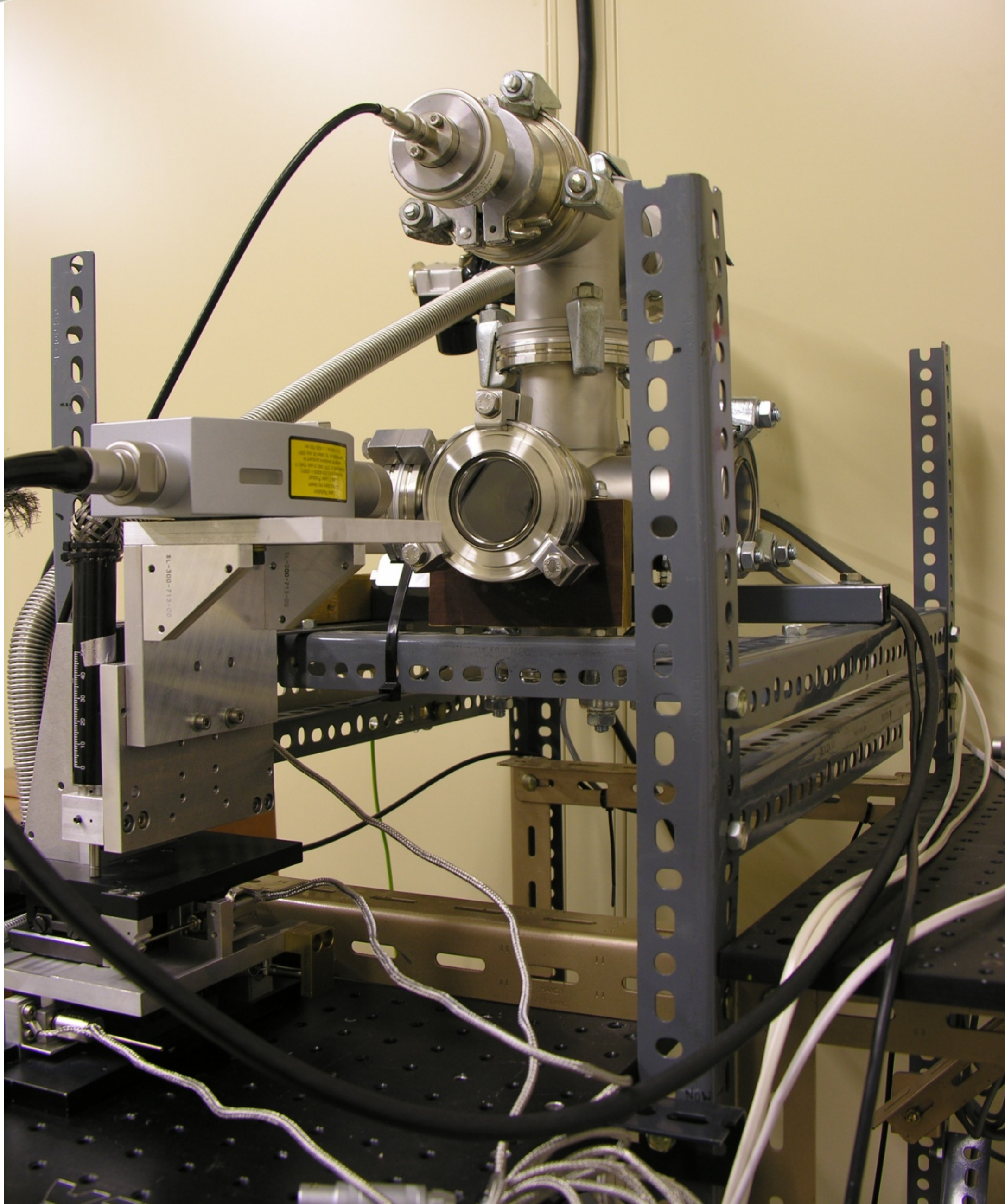

HB2014
54th ICFA Advanced Beam Dynamics Workshop on High-Intensity, High Brightness and High Power Hadron Beams
East Lansing, MI
10-14 November 2014

Solids

One of the main issues for the materials (solids) used in the accelerators and target systems (beam windows, beam dumps, collimators, targets, pipes for contained liquid/powder jets, etc.) is the magnitude and the rate of change of deposited energy density (EDD).

Thermal Stress ~ $\alpha E \Delta T/(1-\nu)$ **$\Delta T = EDD/Cp$**

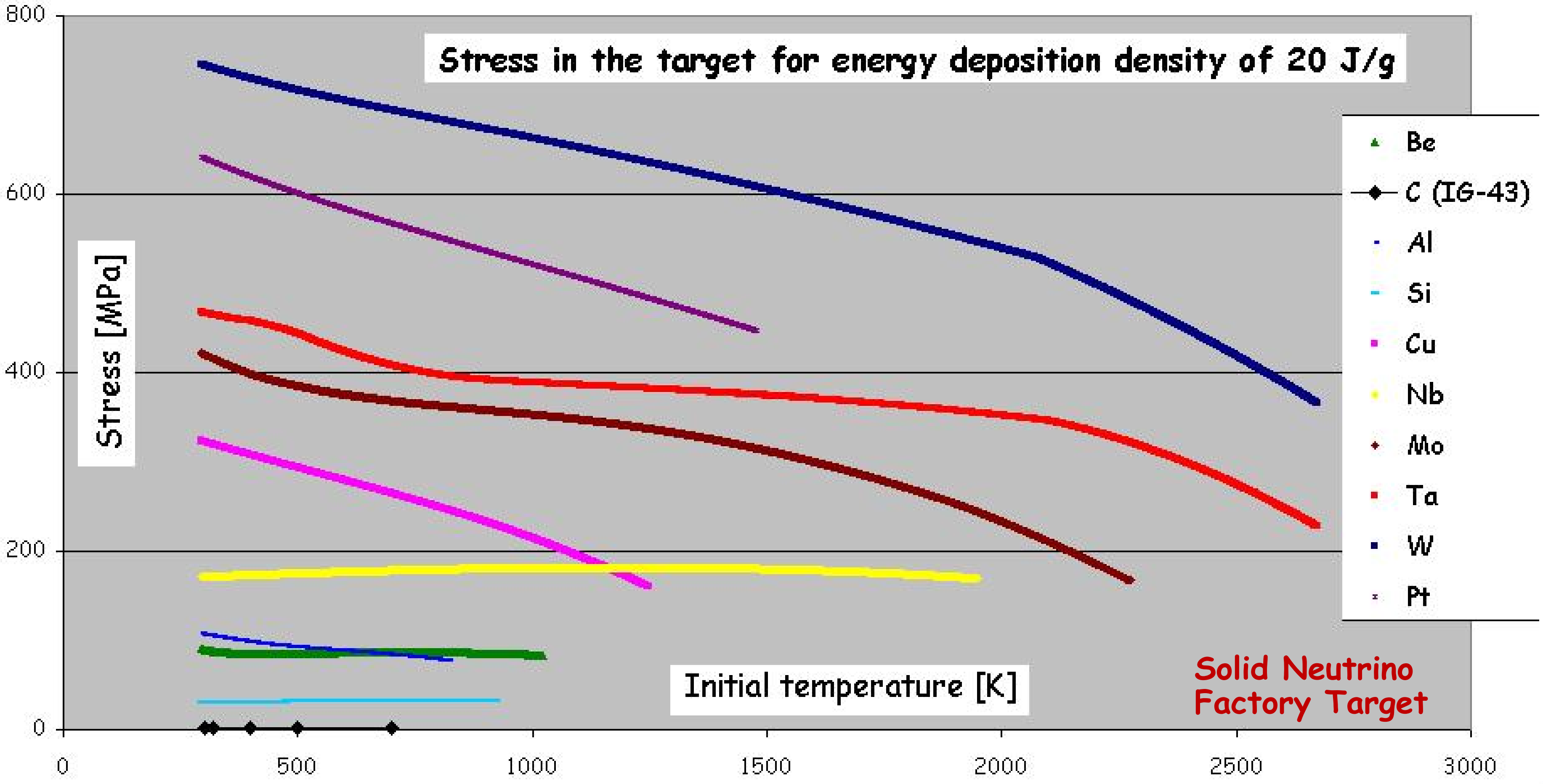

How to minimise the effect of thermal stress?

TARGETRY CHALLENGES AT MEGAWATT PROTON ACCELERATOR FACILITIES *

P. Hurh†, K. Ammigan, B. Hartsell, R. Tschirhart, FNAL, Batavia, IL 60510, USA

- Target/component segmentation
- Avoid stress concentration
- Compressive pre-loading (reducing the tensile stress)
- Beam size/shape optimisation
- Material selection

"Stress quality" factor (one of the possible definitions)

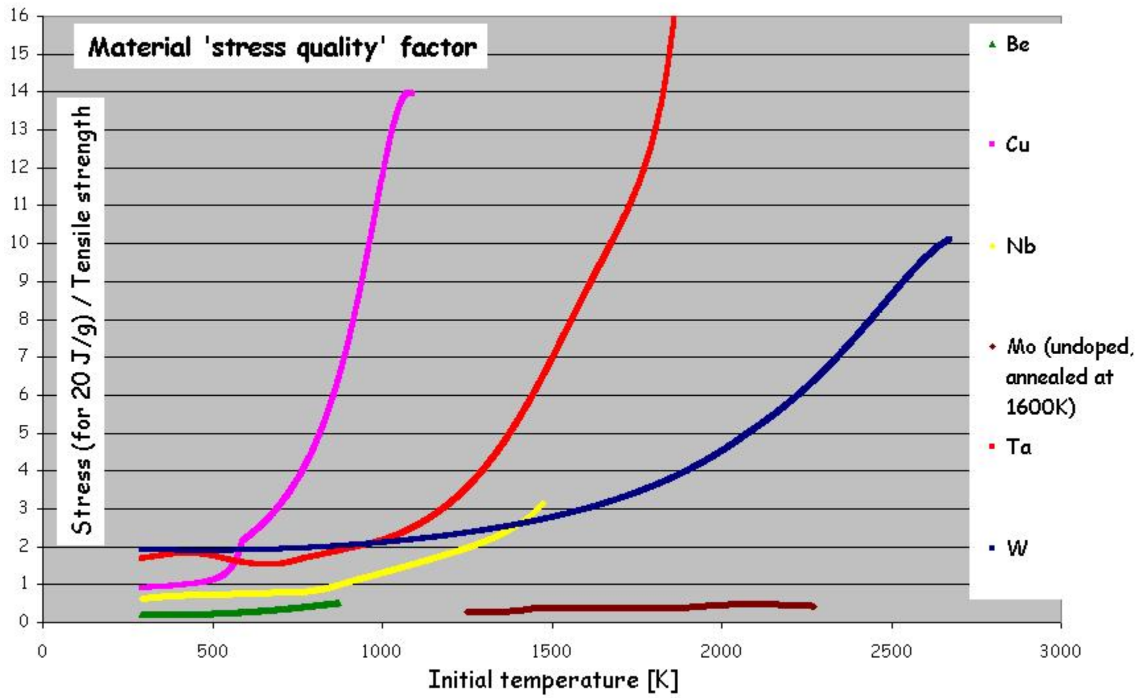

This graph:
quasi-static approximation

Is this approximation valid for short beam pulses (i.e. Neutrino Factory: a few ns long micro-pulses within a micro-second)?

N.B. Carefully check the data (Mo case on this plot)

"Strange" question (on the first glance): Do we know the basic material properties (especially their temperature dependence)?

Stress test Lab @ RAL

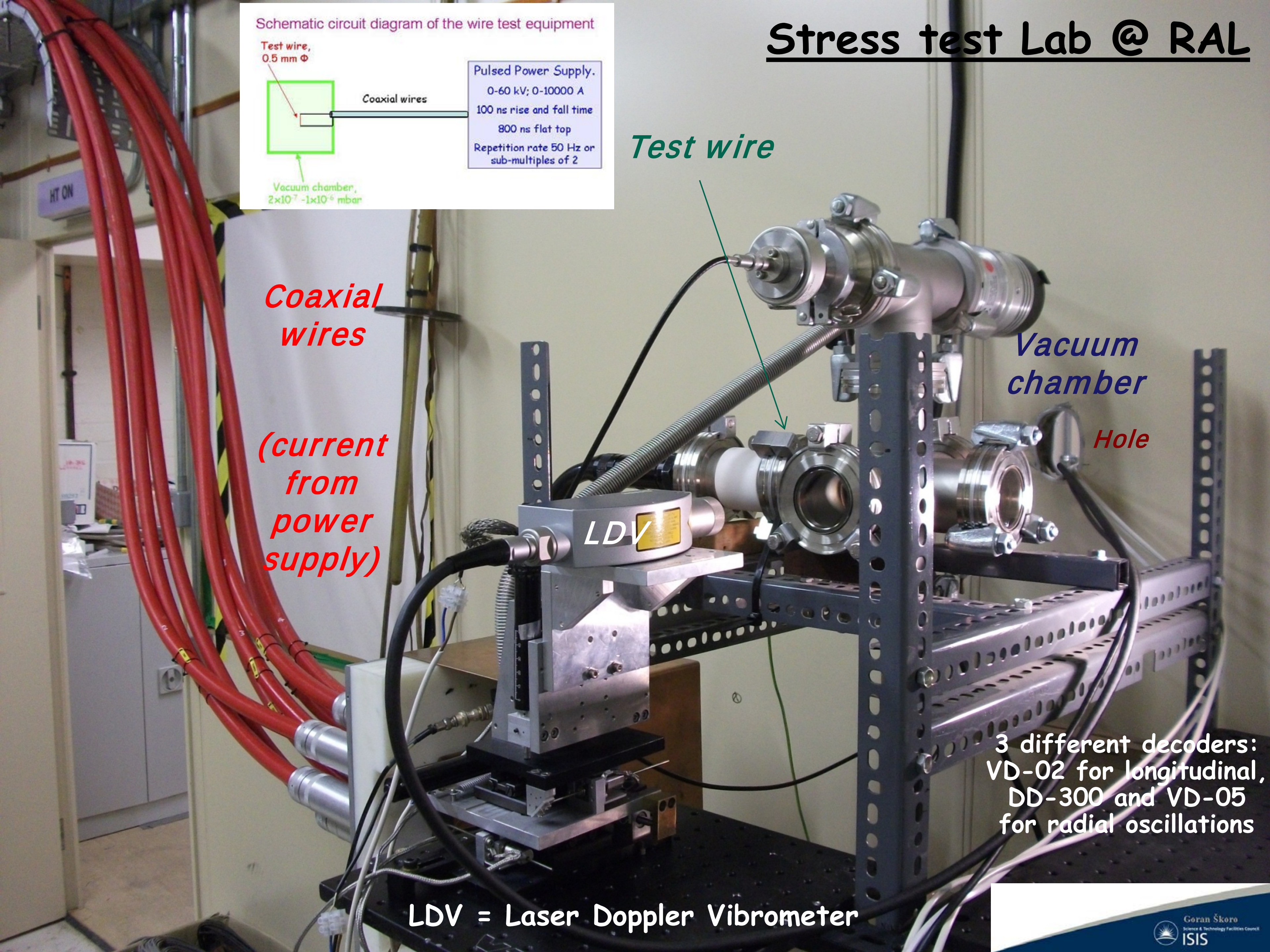

Current pulse – wire tests at RAL

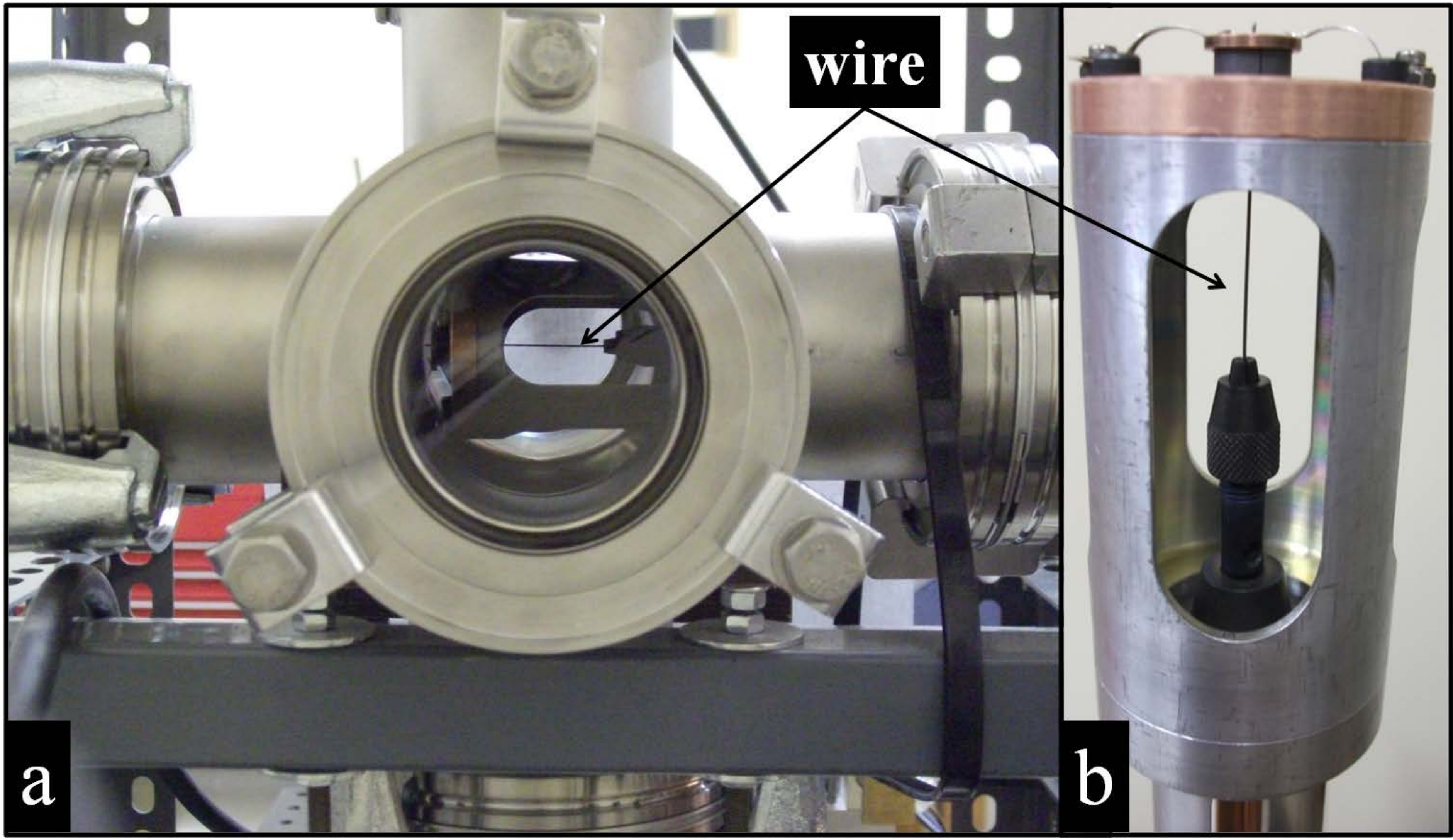

Characteristic frequency of the wire vibration can be used to directly measure Young's modulus of material as a function of temperature.

$$E = \frac{(2\pi f)^2 r^2 \rho}{\zeta^2} \frac{(1+\nu)(1-2\nu)}{(1-\nu)}$$

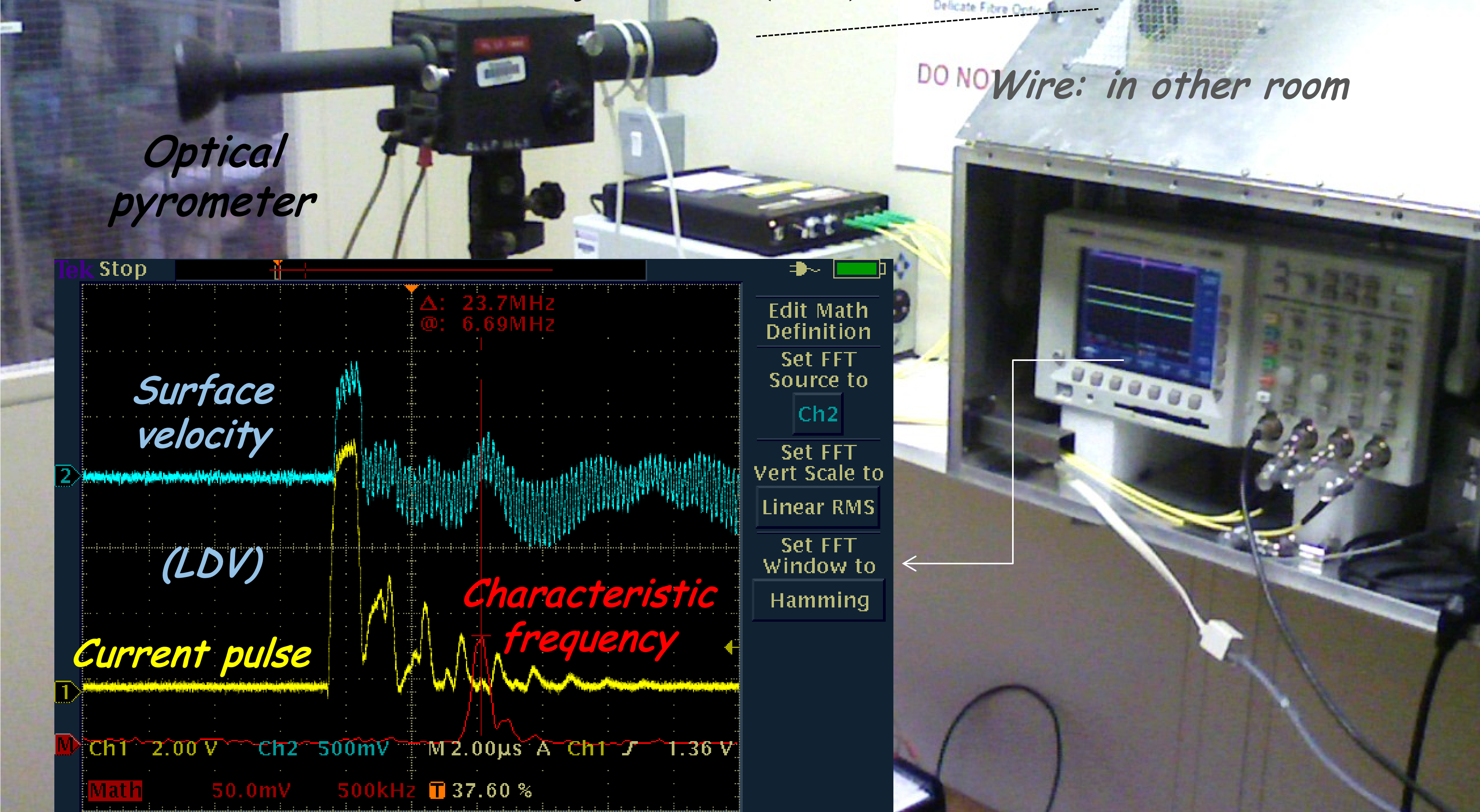

G.P. Škoro et al. / Journal of Nuclear Materials 409 (2011) 40–46

Goran Škoro
ISIS

Young's modulus (tantalum and tungsten)

G.P. Škoro et al. / Journal of Nuclear Materials 409 (2011) 40–46

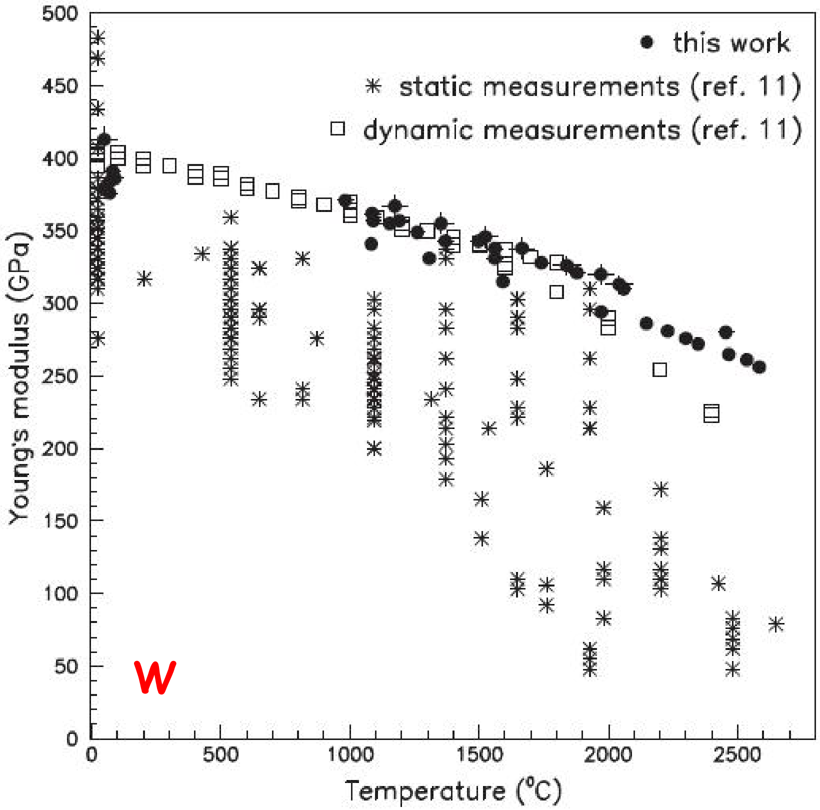

Fig. 10. Comparison between our experimental results and previous results [11] on tungsten Young's modulus.

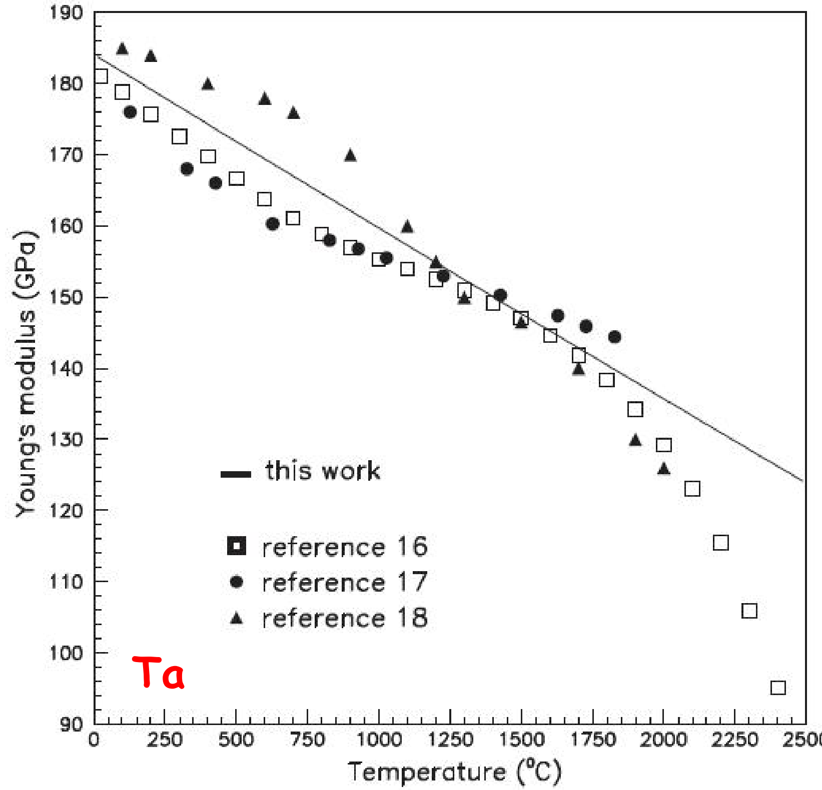

Fig. 13. Comparison between the new experimental data and previous results [16–18] on tantalum Young's modulus.

Significant differences at (very) high temperatures

Direct measurements of material strength

~ 1000 ºC

~ 1400 ºC

~ 1800 ºC

~ 2100 ºC

reduced temperature

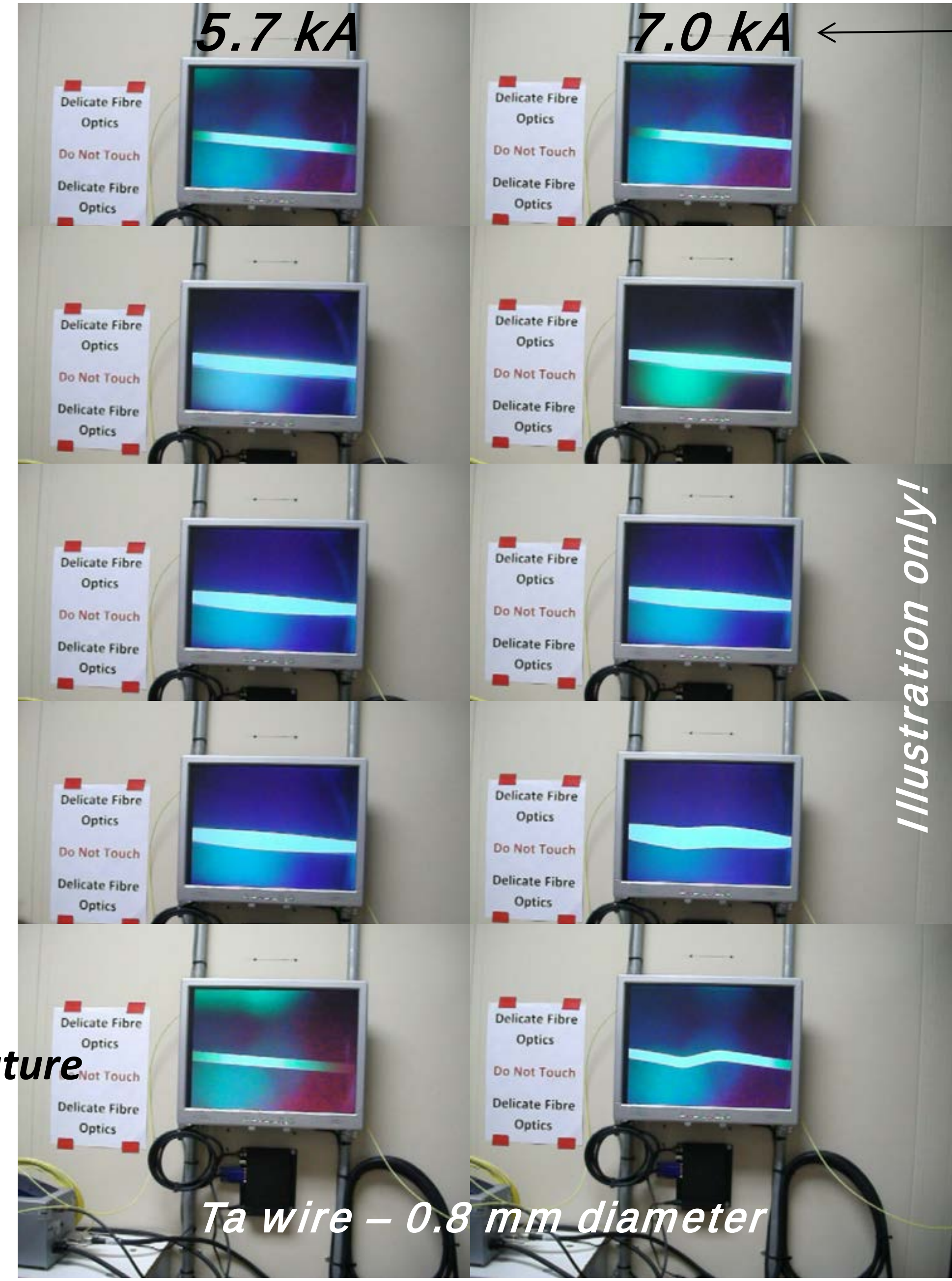

Different stress per pulse

LDV: to monitor wire surface motion (strain rate)

Integrated camera: to monitor the strain of the wire

Elastic-plastic transition: LDV signal becomes very noisy

Stress: calculation (LS-DYNA)

As the beam power increases and the beam pulse length decreases, the estimate of material strength and corresponding lifetime based on simple, quasi-static equations is no longer accurate. In these cases the materials are tested dynamically and they behave differently than under quasi-static loading.

The fundamental material properties and corresponding strength have to be measured under dynamic conditions.

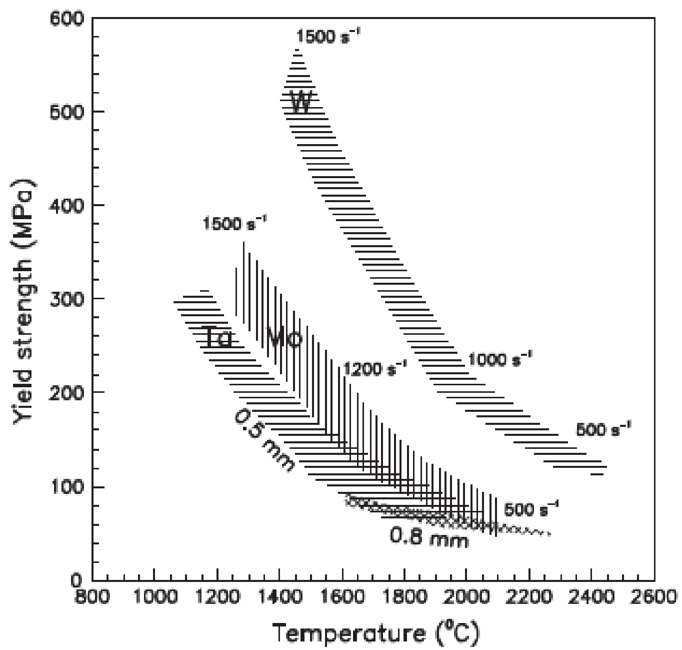

Fig. 2. The yield strength versus peak temperature for tantalum wires of 0.5 and 0.8 mm diameter [5], for tungsten wires of 0.5 mm diameter [5] and for molybdenum wires of 0.5 mm diameter. The upper edge of the bands indicates the stress at which the wire started to bend and the lower edge indicates the stress where the wire was not deformed. The characteristic strain rate values are also shown.

Journal of Nuclear Materials 426 (2012) 45–51

Contents lists available at SciVerse ScienceDirect

Journal of Nuclear Materials

journal homepage: www.elsevier.com/locate/jnucmat

Yield strength of molybdenum, tantalum and tungsten at high strain rates and very high temperatures ☆

G.P. Škoro [a,*], J.R.J. Bennett [b], T.R. Edgecock [b,c], C.N. Booth [a]

[a] Department of Physics and Astronomy, University of Sheffield, Sheffield S3 7RH, UK
[b] STFC, Rutherford Appleton Laboratory, Chilton, Didcot, Oxon OX11 0QX, UK
[c] University of Huddersfield, Queensgate, Huddersfield HD1 3DH, UK

ARTICLE INFO

Article history:
Received 5 October 2011
Accepted 29 March 2012
Available online 4 April 2012

ABSTRACT

Recently reported results of the high strain rate, high temperature measurements of the yield strength of tantalum and tungsten have been analyzed along with new experimental results on the yield strength of molybdenum. Thin wires are subjected to high stress by passing a short, fast, high current pulse through a thin wire; the amplitude of the current governs the stress and the repetition rate of the pulses determines the temperature of the wire. The highest temperatures reached in the experiments were 2100 °C (for molybdenum), 2250 °C (for tantalum) and 2450 °C (for tungsten). The strain-rates in the tests were in the range from 500 to 1500 s^{-1}. The parameters for the constitutive equation developed by Zerilli and Armstrong have been determined from the experimental data and the results have been compared with the data obtained at lower temperatures. An exceptionally good fit is obtained for the deformation of tungsten.

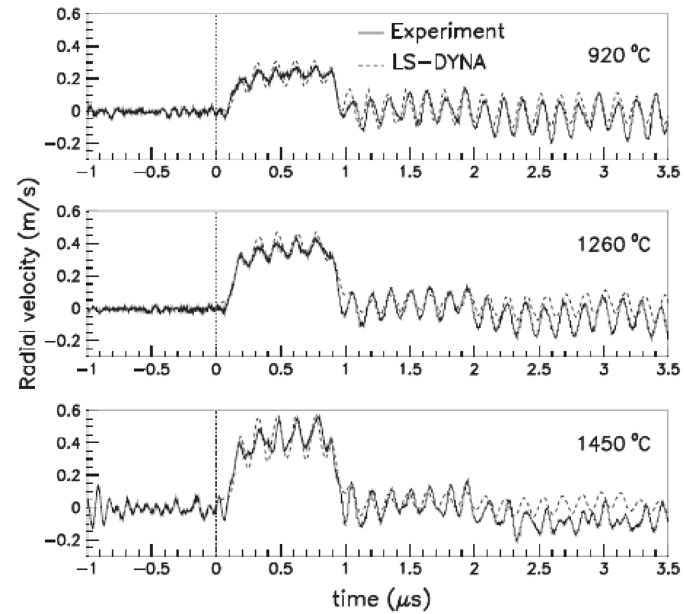

Fig. 1. The measured and calculated radial velocity of a 0.5 mm diameter tungsten wire at peak temperatures of 920, 1260 and 1450 °C [5].

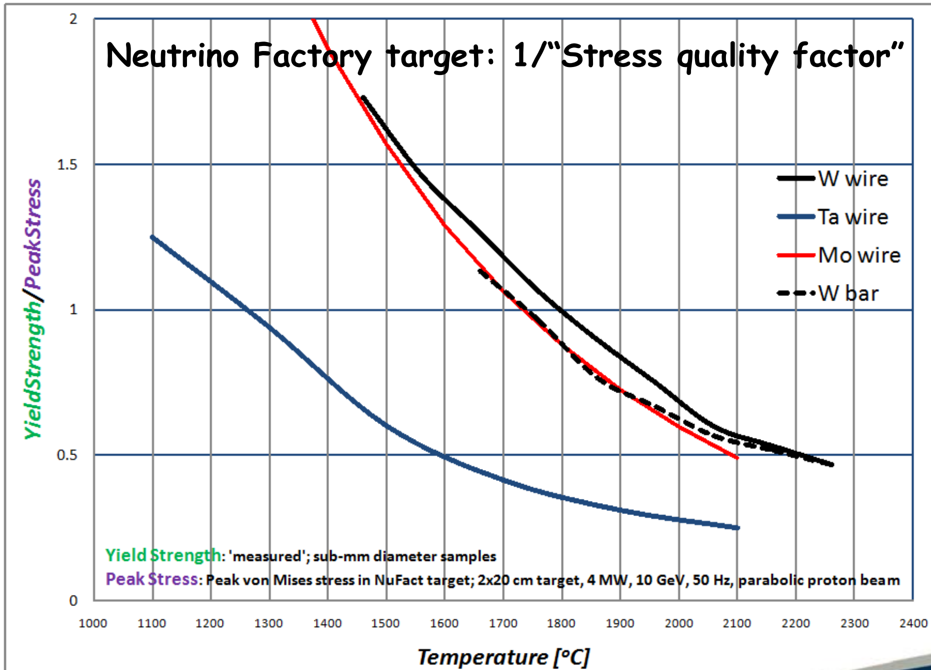

PAUL S. FOLLANSBEE

Analysis of Deformation Kinetics in Seven Body-Centered-Cubic Pure Metals Using a Two-Obstacle Model

METALLURGICAL AND MATERIALS TRANSACTIONS A

VOLUME 41A, DECEMBER 2010—3081

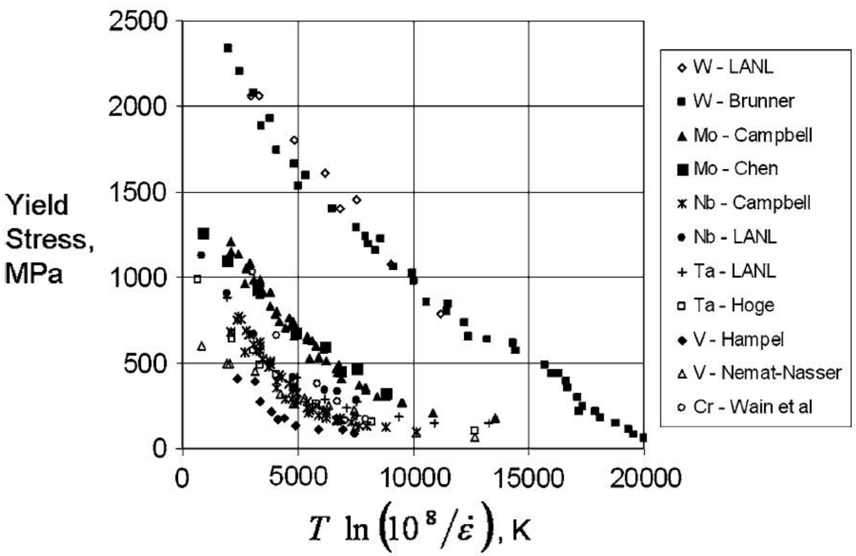

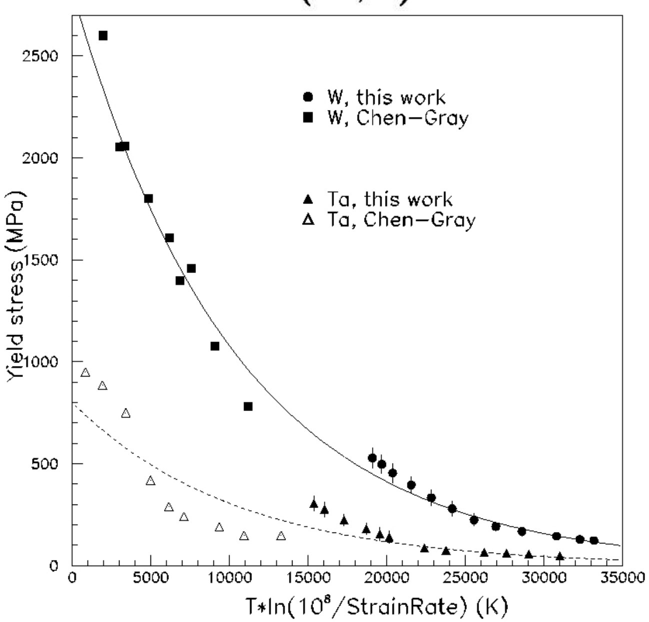

Figure 1 shows raw data for W, Mo, Nb, Ta, V, and Cr, and Figure 2 shows the data set for Fe considered here. The yield stress in both figures is plotted against

$$T \ln(\dot{\varepsilon}_0/\dot{\varepsilon}) \qquad [1]$$

which is a commonly used combination of temperature, T, and strain rate, $\dot{\varepsilon}$, for thermally activated processes. For all of the data, a value of $\dot{\varepsilon}_0 = 10^8\ s^{-1}$ is used.

When plotted according to Eq. [1], several common features emerge. First, most of the data sets (excluding W and Cr) show a curvature characterized by a decreasingly negative slope with increasing values of the abscissa. Second, at low values of the abscissa in some metals (*e.g.*, Fe), there appears to be a maximum (saturation) stress observed with no temperature dependence as temperature is further decreased or strain rate increased.

This latter behavior has been attributed to the initiation of deformation twinning.[23,30,31] These data points will not be included in the analysis presented here.

Included in many of the references in Tables I and II is model analysis. The common approach is to seek a single thermally activated process represented by an expression that is a variant of $\sigma \propto T \ln(\dot{\varepsilon}_0/\dot{\varepsilon})$.[16,24] Others have recognized the two extreme behaviors (low T and high $\dot{\varepsilon}$ *vs* high T and low $\dot{\varepsilon}$) and have proposed separate deformation mechanisms active in these regimes.[15] The model presented subsequently does not differ significantly from these approaches, although it does attempt to recognize the coexistence of two distinct obstacles restricting dislocation motion and contributing to defining the resulting deformation kinetics over a wide range of conditions

… "collaboration" with material scientists essential

Fatigue

Traditional view: solid targets safe up to only 50-70 J/g deposited energy (below 1-2 MW beam power)

Empirical evidence:some materials survive 500-1000 J/g,
⇒ May survive 4 MW if rep rate ≥ 10 Hz.

Solid targets in FNAL p-bar source: "damaged but not failed" for peak energy deposition of 1500 J/g!!!

Our fatigue / lifetime tests: Mo has issues…

Tantalum cladded tungsten target(s): HIP procedure,…

Radiation damage…

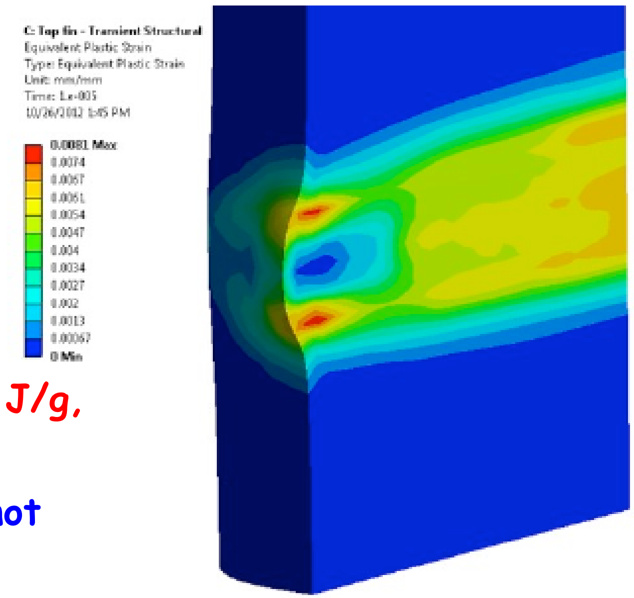

Figure 1: Simulation of 120 GeV protons (1.03e13 ppp, 0.16 x 0.22 mm sigma) on Be fin showing plastic strain.

Testing of prototypical target designs and materials with actual high intensity beam is necessary to validate modeling and simulation as well as material properties and failure criteria for the candidate materials. The latter is important because, at these load rates the material behavior is strain rate dependent and also because the compressive nature of the stress arising from the beam pulse may not "fail" the target material even if yielding occurs. Figure 1 shows simulation results for 120 GeV protons on beryllium. Although plastic deformation occurs, the target is intact for the next pulse and, in fact, the elastic residual tensile strain left after the first pulse reduces the peak stress from subsequent pulses. These results match anecdotal observations of Be components at Fermilab's anti-proton source, but need to be more rigorously tested in an instrumented beam test. Ideally, these beam tests would also be conducted on irradiated materials to account for radiation damage effects.

TARGETRY CHALLENGES AT MEGAWATT PROTON ACCELERATOR FACILITIES *

P. Hurh†, K. Ammigan, B. Hartsell, R. Tschirhart, FNAL, Batavia, IL 60510, USA

Proton Beam Window (PBW) for ESS

J. Wolters[1], M. Butzek[1], B. Laatsch[1], Y. Beßler[1], G. Natour[1], P. Nilsson[2], P. Sabbagh[2]

[1]Forschungszentrum Jülich GmbH, Jülich, Germany; [2]European Spallation Source ESS, Lund, Sweden

JÜLICH FORSCHUNGSZENTRUM

SPONSORED BY THE
EUROPEAN SPALLATION SOURCE
Federal Ministry of Education and Research

- the PBW separates the accelerator vacuum from the helium atmosphere in the target room at 1 bar
- Al6061-T6 is the preferred material for the PBW
- helium at 10 bar is used for PBW cooling (customer request: no water cooling!)
- Maximum time-averaged heat deposition @ beam center: 0.5 kW/cm³
- pulsed operation at 14 Hz & beam trips => risk of fatigue

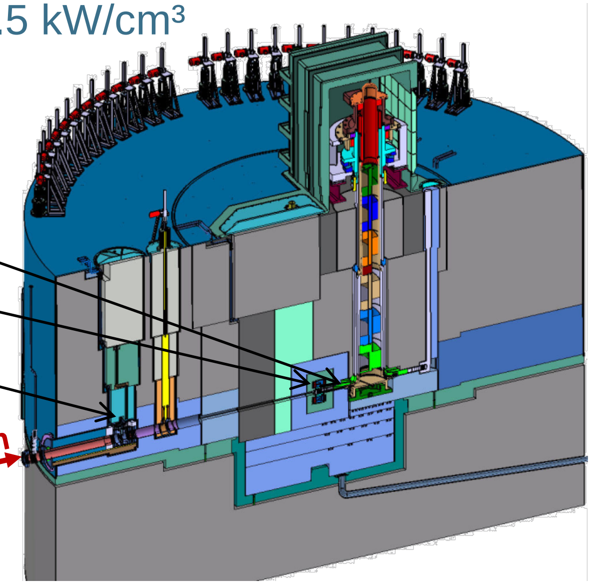

New concept: panpipe design

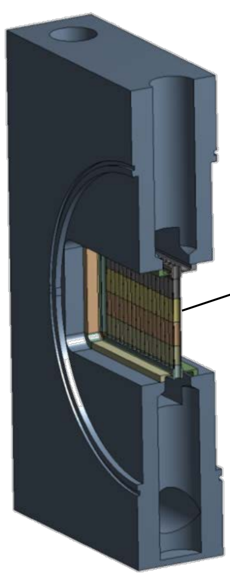

Central Institute for Engineering, Electronics and Analytics | ZEA

Engineering und Technology | ZEA-1
Technology for World-Class Research

Thermo-mechanical design of the PBW

JÜLICH FORSCHUNGSZENTRUM

SPONSORED BY THE

EUROPEAN SPALLATION SOURCE

Federal Ministry of Education and Research

coolant velocity, m/s

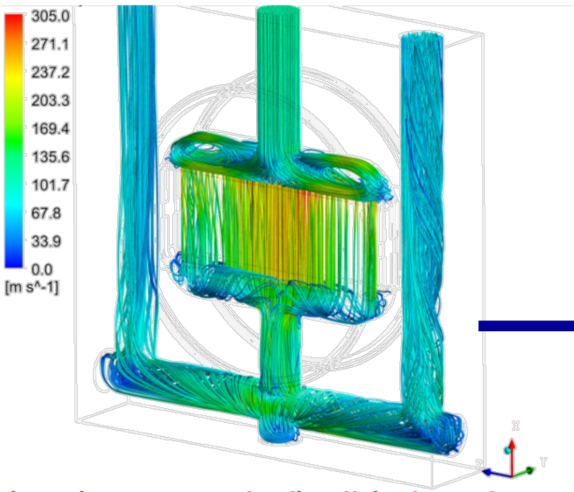

temperature, °C

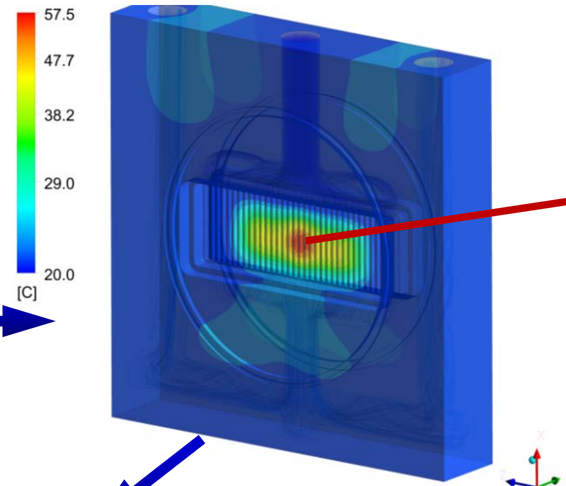

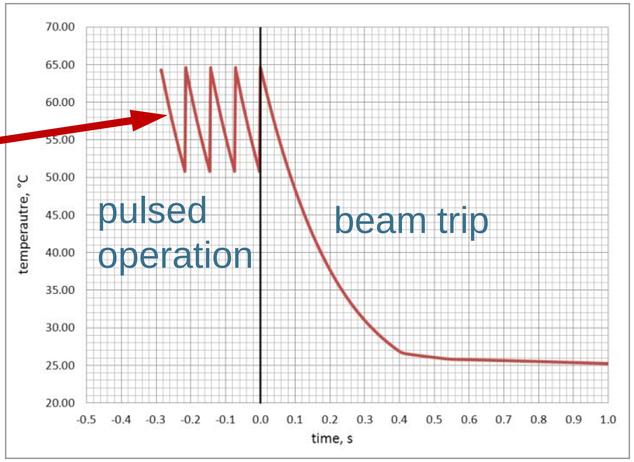

local stresses in flexible interface, MPa

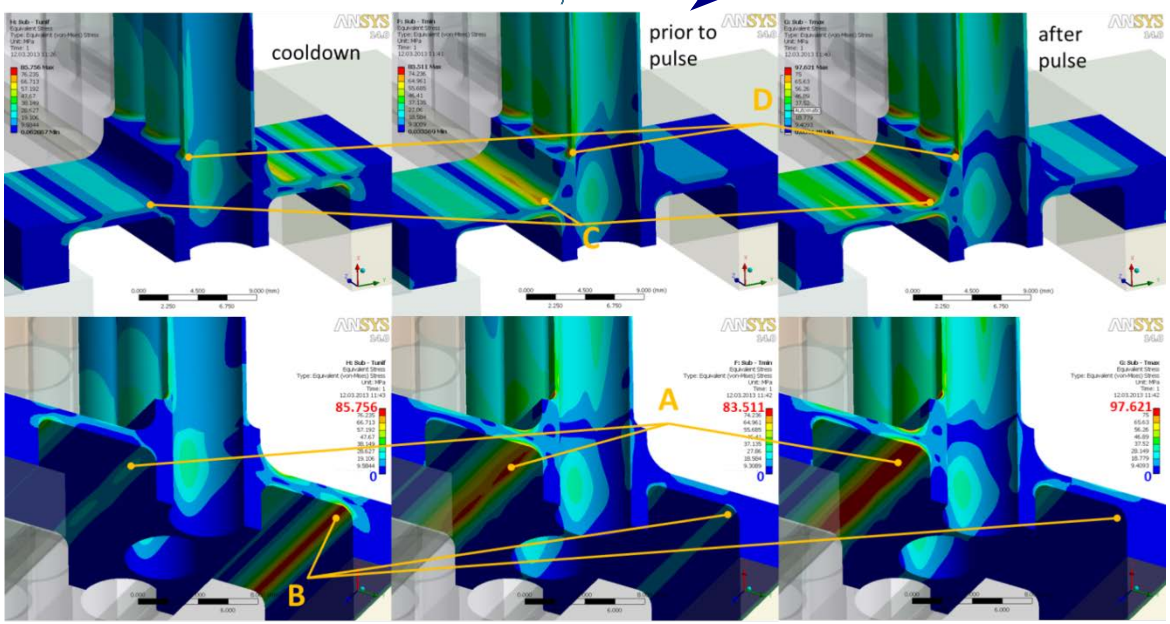

fatigue design	degree of utilization [%]			
point	A	B	C	D
pulsed operation	25.6	27.4	19.5	5.9
beam trips	45.3	51.5	45.9	16.8
total	70.0	78.9	65.4	22.7

Central Institute for Engineering, Electronics and Analytics | ZEA

TÜVRheinland ZERTIFIZIERT Management System ISO 9001:2008 www.tuv.com ID 9108611694

Engineering und Technology | ZEA-1
Technology for World-Class Research

Journal of Nuclear Materials 398 (2010) 93–99

Contents lists available at ScienceDirect

Journal of Nuclear Materials

journal homepage: www.elsevier.com/locate/jnucmat

Study on low activation decoupler material for MW-class spallation neutron sources

M. Harada *, M. Teshigawara, F. Maekawa, M. Futakawa

Materials and Life Science Division, J-PARC Center, Japan Atomic Energy Agency, Tokai-mura, Naka-gun, Ibaraki-ken 319-1195, Japan

A B S T R A C T

The Japan Spallation Neutron Source (JSNS) at the Japan Proton Accelerator Research Complex (J-PARC) has started its operation on May 30, 2008. The Ag–In–Cd (AIC) alloy was adopted as a decoupler material for two decoupled moderators. A high decoupling energy at 1 eV was for the first time achieved in MW-class spallation neutron sources due to the adoption of the AIC alloy. Although the AIC decoupler is superior in the neutronic performance, it has a demerit in high residual radioactivity due to production of Ag-110 m (half life: 250 days) and Ag-108 m (half life: 418 years). To overcome this demerit, we studied on possibilities of a low activation decoupler material with high decoupling energy as the AIC alloy, that is, Au–In–Cd (AuIC) alloy. Neutronic performance of this material was investigated by using neutronics calculations. As a result, it was found that the AuIC decoupler could provide neutron pulses with almost the same characteristics as those for the AIC decoupler even when the burn-up effects were considered. Excellent low activation property of the AuIC alloy to the AIC alloy was demonstrated by residual radioactivity calculations. On viewpoint of neutronics performance, it was concluded that the AuIC decoupler was available as the substitute of the AIC decoupler.

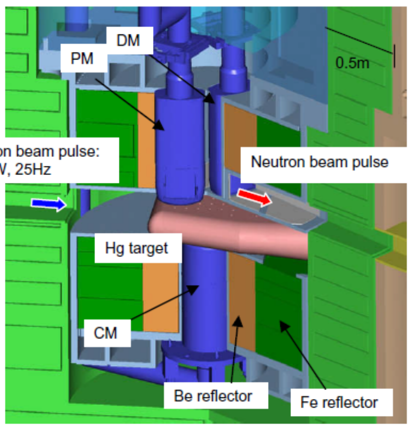

Fig. 1. Schematic view of Target–Moderator–Reflector assembly in JSNS.

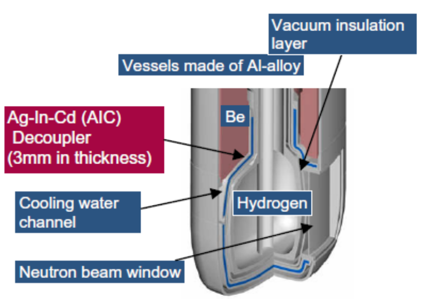

Fig. 2. Schematic view of DM.

For high resolution experiments in the JSNS, the decoupled moderators with higher E_d are desirable. Until recently, a candidate of decoupler material to realize $E_d \sim 1$ eV was only boron (B) provided by boron carbide (B_4C). However, in the intense neutron source, the large helium (He) gas production rate due to the $^{10}B(n, \alpha)$ reaction leads to serious problems (swelling). In addition, E_d of B_4C changes according to a burn-up of B. Therefore, such a candidate is limited to a decoupler material based on the (n, γ)

interesting issue at high power...

Journal of Nuclear Materials 431 (2012) 218–223

Contents lists available at SciVerse ScienceDirect

Journal of Nuclear Materials

journal homepage: www.elsevier.com/locate/jnucmat

Development status of low activation ternary Au–In–Cd alloy decoupler for a MW class spallation neutron source
1st Production of Au–In–Cd alloy

Motoki Ooi *, Makoto Teshigawara, Takashi Wakui, Tsuyoshi Nishi, Masahide Harada, Fujio Maekawa, Masatoshi Futakawa

Japan Atomic Energy Agency, Tokai-mura, Naka-gun, Ibaraki 319-1195, Japan

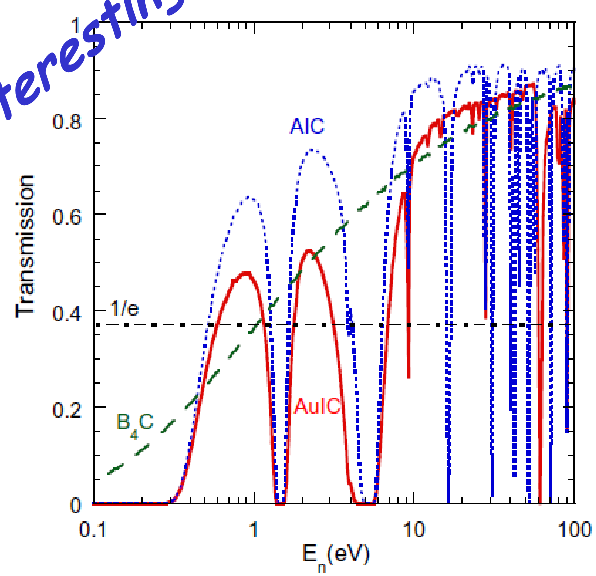

Fig. 3. Neutron transmission of AuIC, AIC and B_4C (E_d = 1 eV).

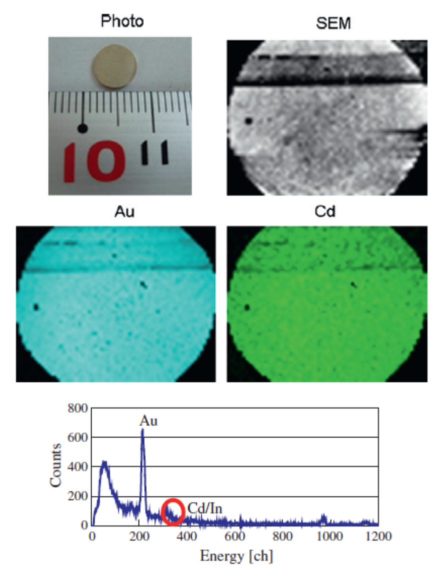

Fig. 6. Results of EDX area scan of the Au–In–Cd alloy. Upper-left panel: photograph of the sample; upper-right panel: SEM image; middle-left panel: Au distribution; middle-right panel: Cd distribution; bottom image: EDX spectrum.

Liquids

Project members:

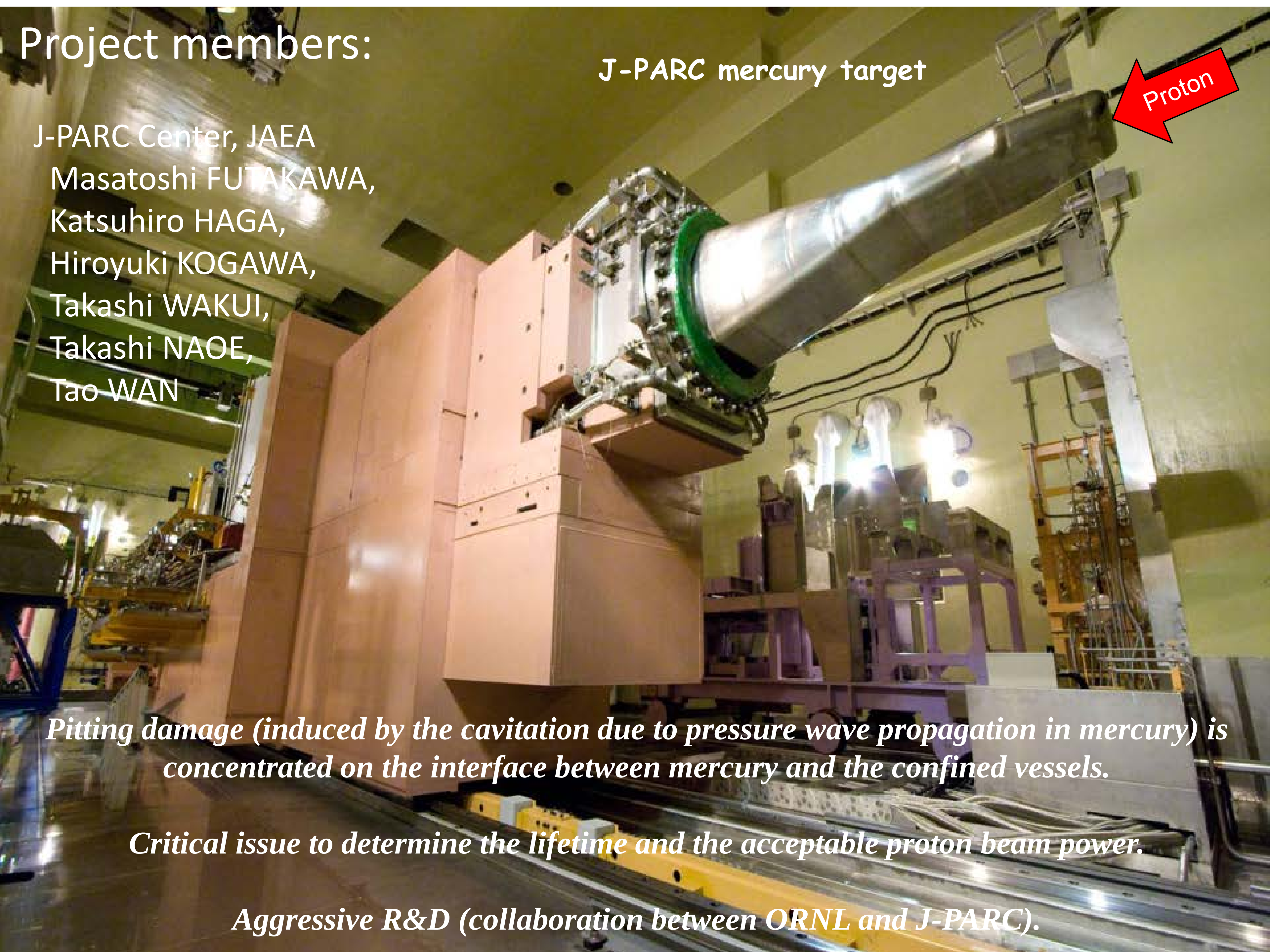

J-PARC Center, JAEA
Masatoshi FUTAKAWA,
Katsuhiro HAGA,
Hiroyuki KOGAWA,
Takashi WAKUI,
Takashi NAOE,
Tao WAN

Pitting damage (induced by the cavitation due to pressure wave propagation in mercury) is concentrated on the interface between mercury and the confined vessels.

Critical issue to determine the lifetime and the acceptable proton beam power.

Aggressive R&D (collaboration between ORNL and J-PARC).

The cavitation damage occurs due to the collapse of the cavitation bubble near the vessel wall. The cavitation bubble is produced by the negative pressure which is generated by the rapid expansion of the target vessel wall caused by the load of the pressure waves.
Reduction of the pressure waves is one of technique to reduce the cavitation damage.
A helium gas microbubble injection system was installed in the J-PARC mercury target system to reduce the pressure wave and it has been operated since November in 2012.
After improving the ventilation during the maintenance period in 2013, the injected gas flow rate has been increased 4times than ever with recovery of the mercury flow rate. This leaded to improve the pressure wave reduction rate up to 1/3.

Detection of the vibration induced by proton beam injection

In-situ measuring system

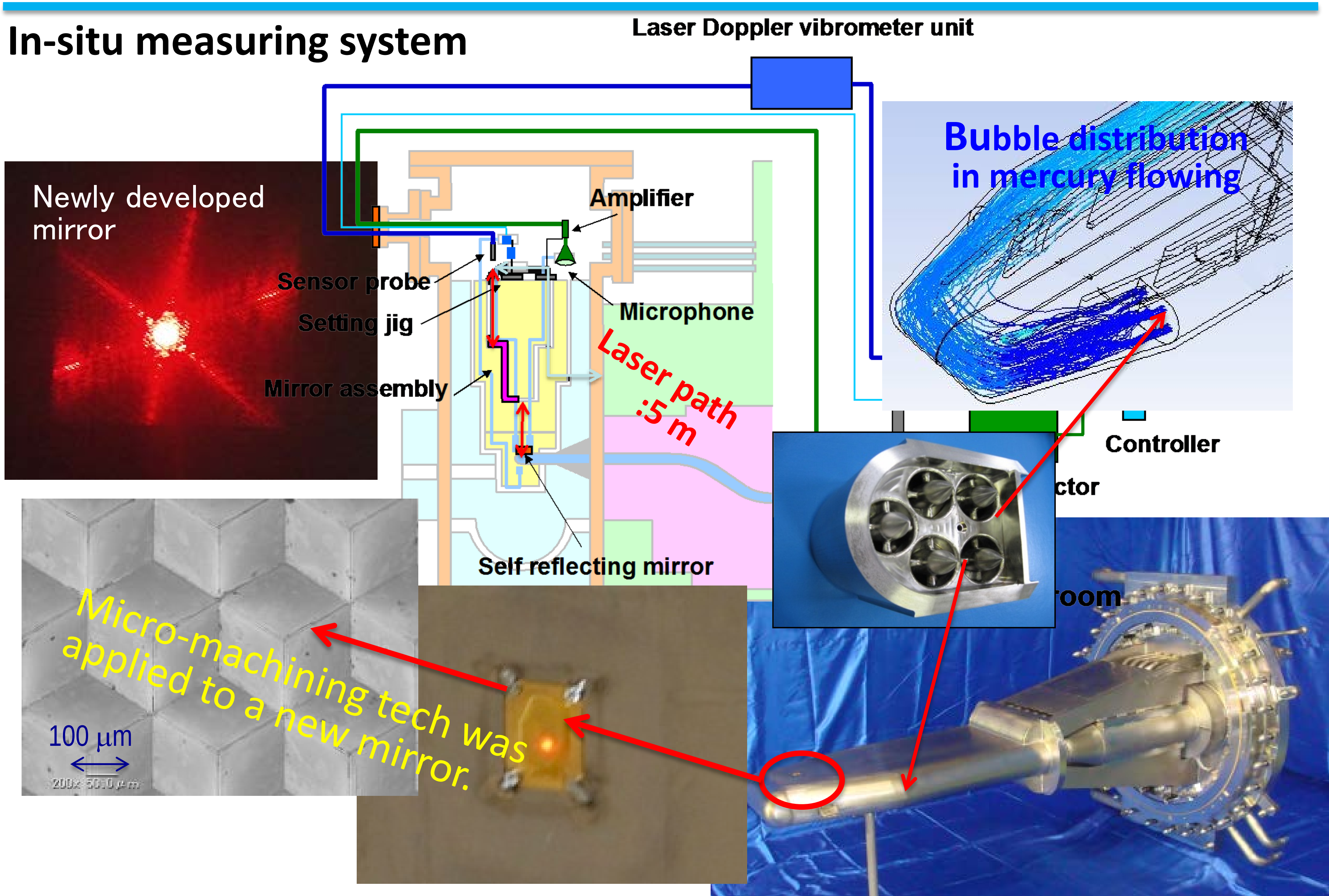

Bubbling mitigation effect on pressure wave responses

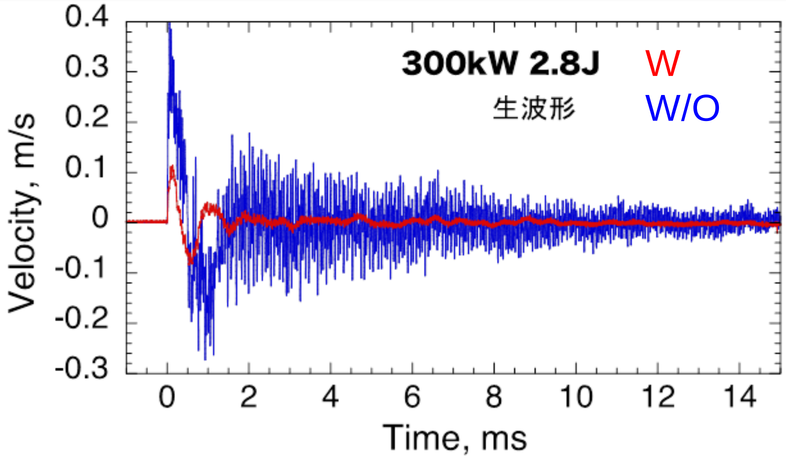

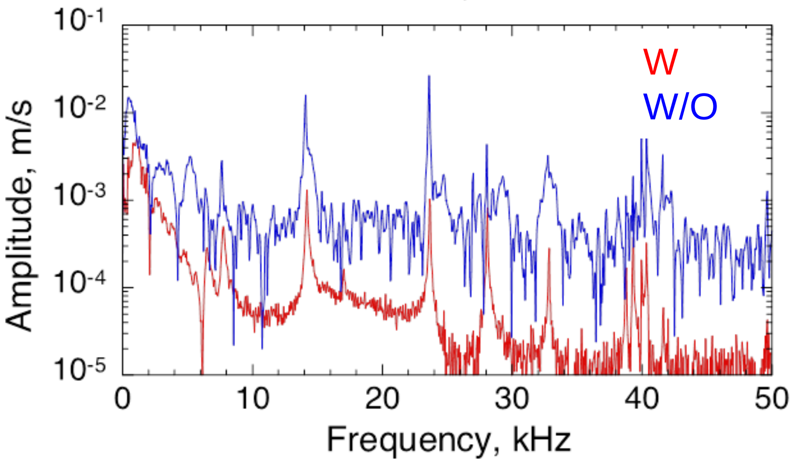

周波数によらず全体的に低下する

The peaks of spectrum were reduced clearly by bubbles injection regardless of frequency.

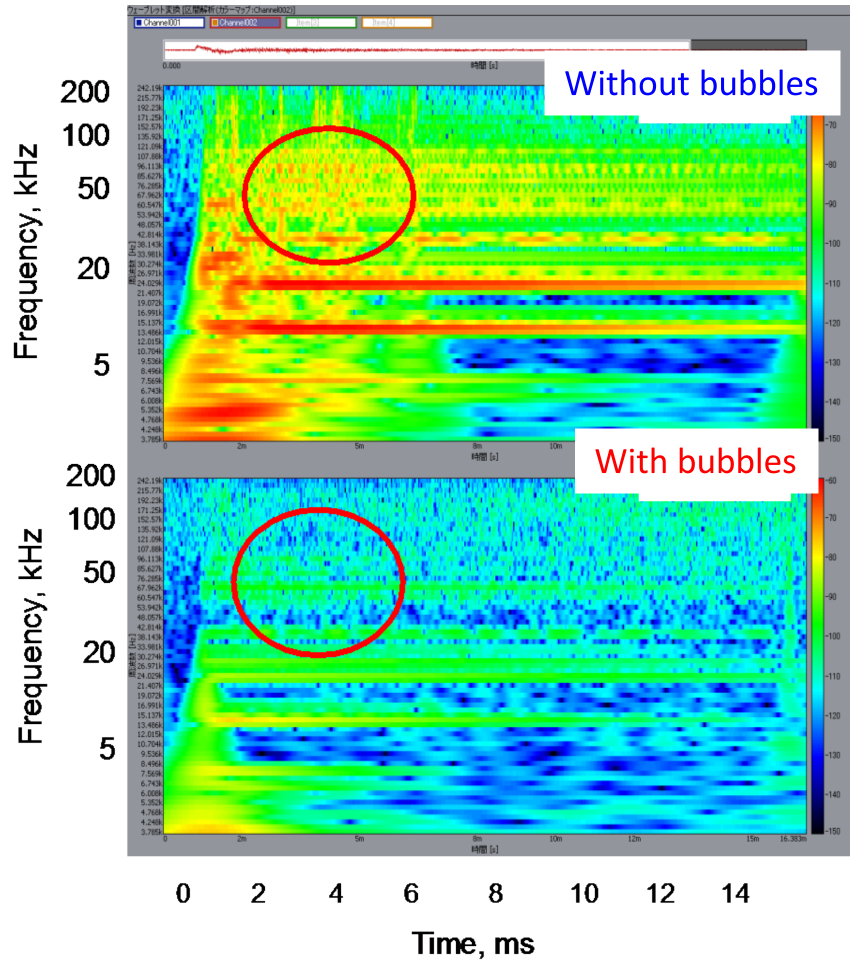

Higher freq. components, related with cavitation phenomena, were sufficiently mitigated.

Something between solid and liquid?

Fluidised tungsten powder technology

RAL HPTG:

Chris Densham, Tristan Davenne, Mike Fitton, Peter Loveridge, Otto Caretta, Matt Rooney, Dan Wilcox, Joe O'Dell

Motivation: Material already fragmented; no cavitation; thermal stress contained within grains; target can be continuously reformed; can be 'pumped' away, externally cooled and recirculated.

- Potential solution for applications requiring highest pulsed beam powers e.g. alternative to Neutrino Factory liquid mercury jet
- Pneumatically (helium) recirculated tungsten powder

1. Suction / Lift
2. Load Hopper
3. Pressurise Hopper
4. Powder Ejection and Observation

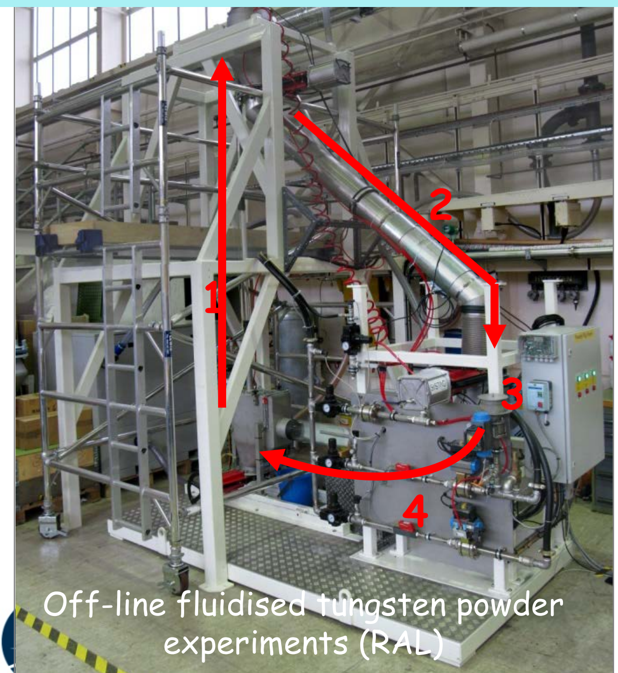

Off-line fluidised tungsten powder experiments (RAL)

In-beam experiment

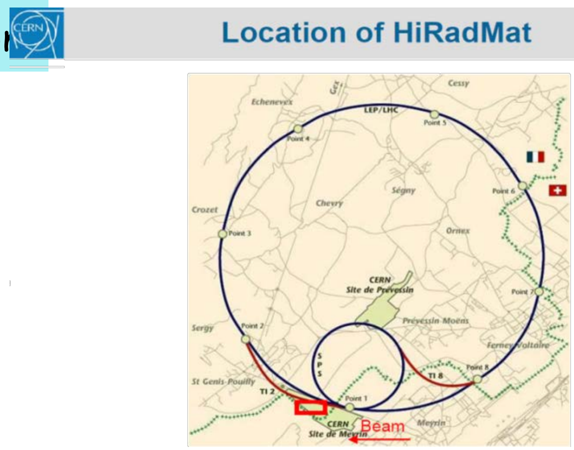

HiRadMat Beam Parameters:

A high-intensity beam pulse from SPS of proton or ion beams is directed to the HiRadMat facility in parasitic mode, using the existing fast extraction channel to LHC..

Beam Energy 440 GeV
Pulse Energy up to 3.4 MJ
Bunch intensity $3.0 \cdot 10^{9}$ to $1.7 \cdot 10^{11}$ protons
Number of bunches 1 to 288
Maximum pulse intensity $4.9 \cdot 10^{13}$ protons
Bunch length 11.24 cm
Bunch spacing 25, 50, 75 or 150 ns
Pulse length 7.2 μs
Beam size at target variable around 1 mm^2

HiRadMat: very interesting and important results (characterisation of novel, more robust materials for beam collimation at higher power).

In beam tests at CERN (in collaboration with Ilias Efthymiopoulos, Nikos Charitonidis (CERN), Rachel Salter, Jennifer Wark (RAL))

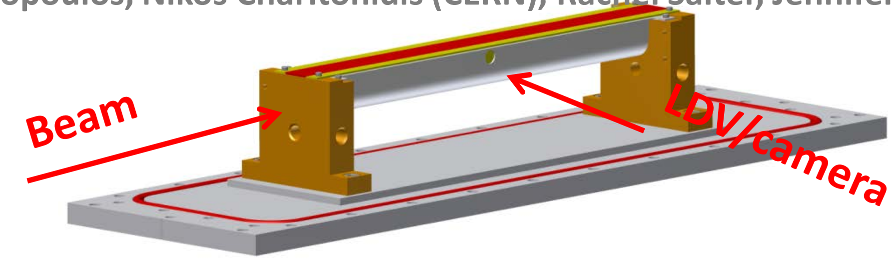

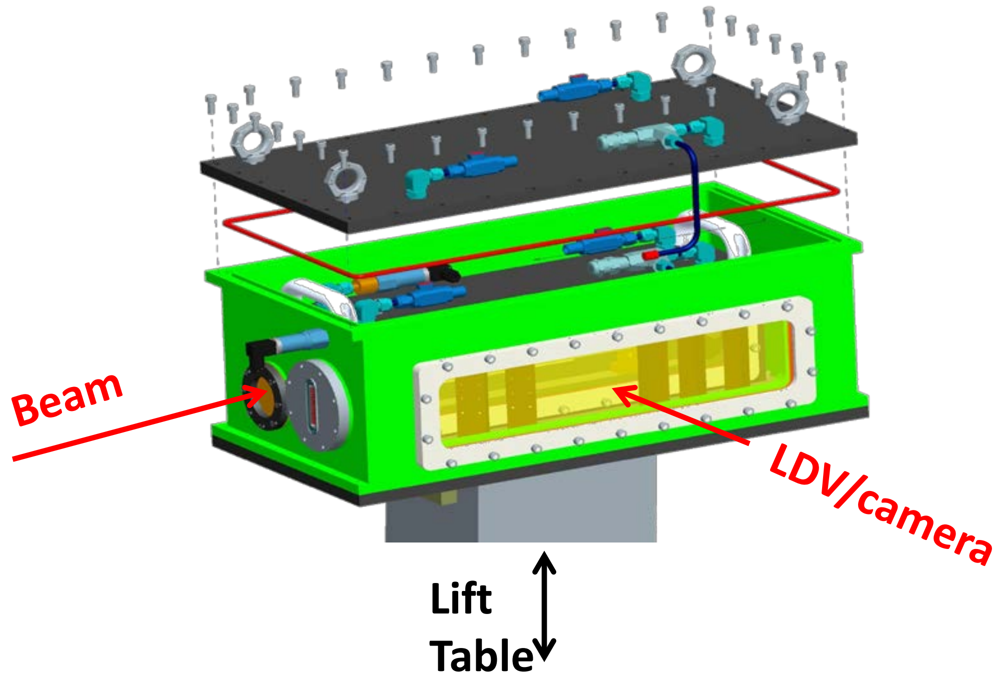

- Tungsten powder sample in an open trough configuration
- Helium environment
- Two layers of containment with optical windows to view the sample
- Remote diagnostics via LDV and high-speed camera

1. Is stress wave propagation through the powder significant?
2. How severe is beam induced gas expansion as a mechanism for eruption?

Proposed beam induced gas expansion mechanism:

- Beam interaction causes sudden heating of powder sample
- Gas pressure rises as a result of rapid heating
- Gas expands and escapes through powder to the surface
- If temperature and pressure is high enough particles can be lifted by aerodynamic force applied by the escaping gas
- It was postulated that a threshold exists for powder eruption:

  -below which the expanding gas escapes without disrupting the powder

  -above which the expanding gas lifts powder grains as it escapes through the powder

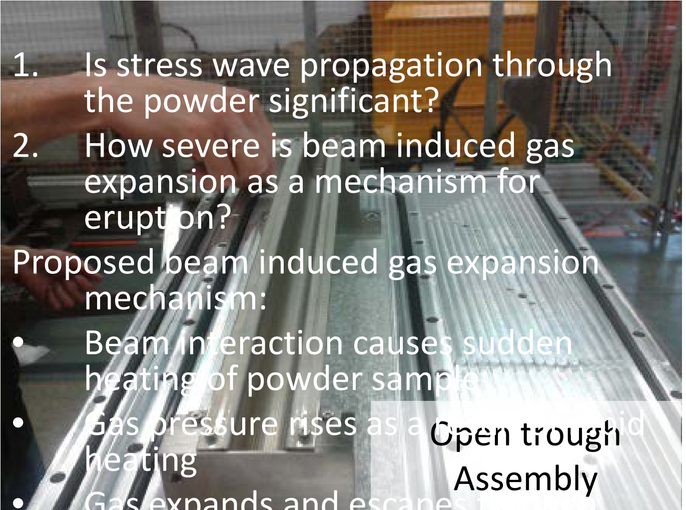

Open trough Assembly

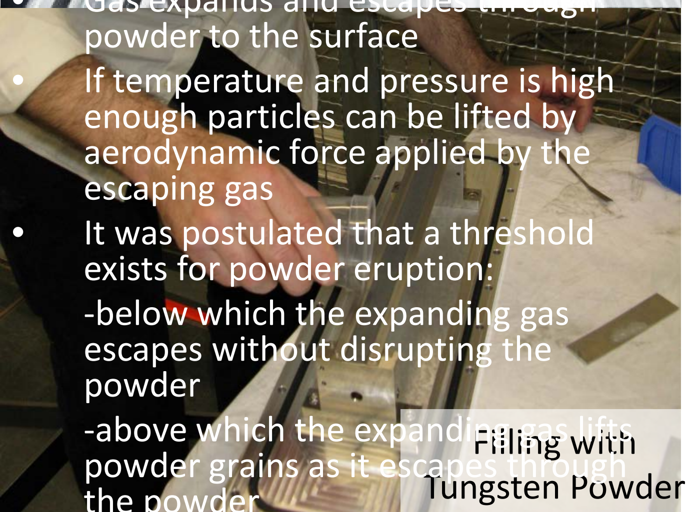

Filling with Tungsten Powder

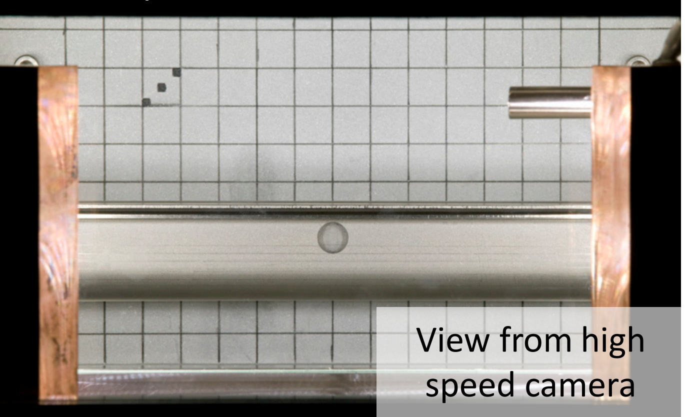

View from high speed camera

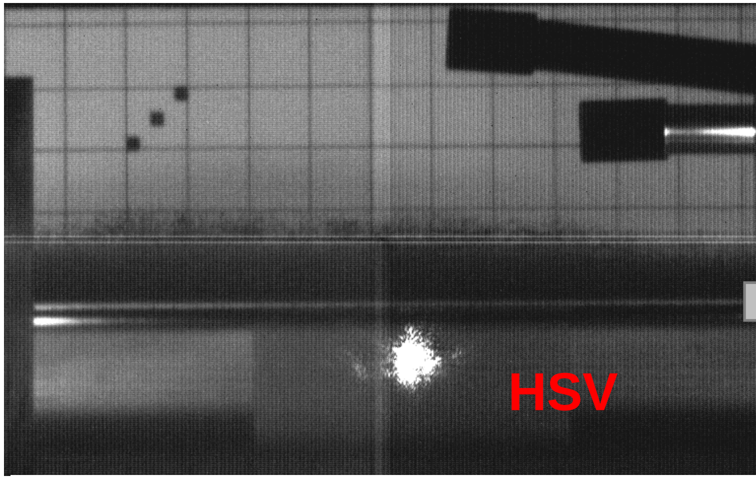

Shot #8, 1.75e11 protons
Note: nice uniform lift

Lift height correlates with deposited energy

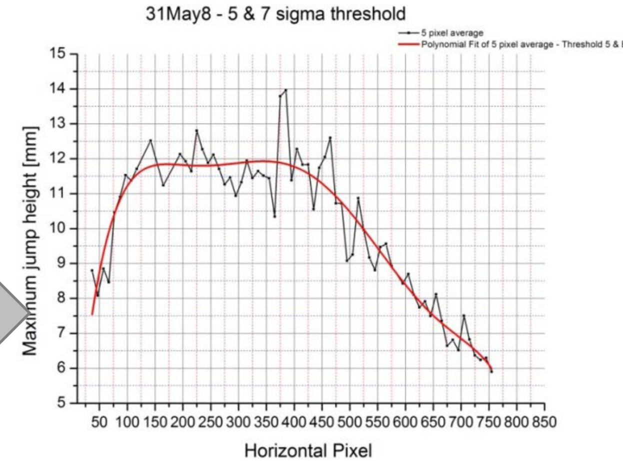

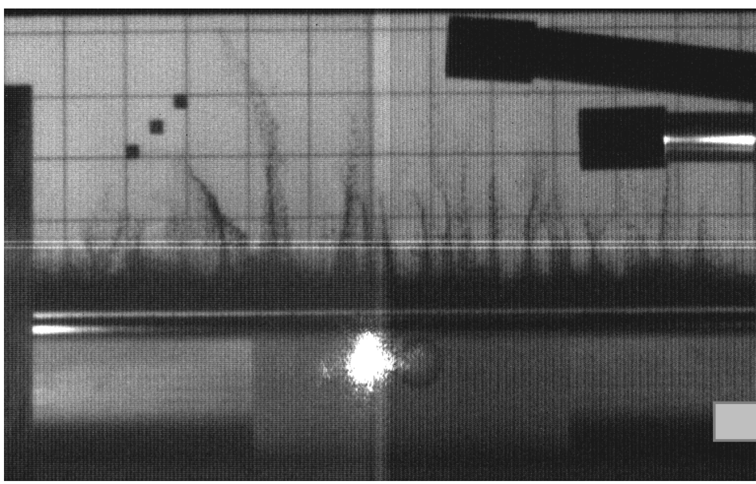

Shot #9, 1.85e11 protons
Note: filaments due to disrupted surface!

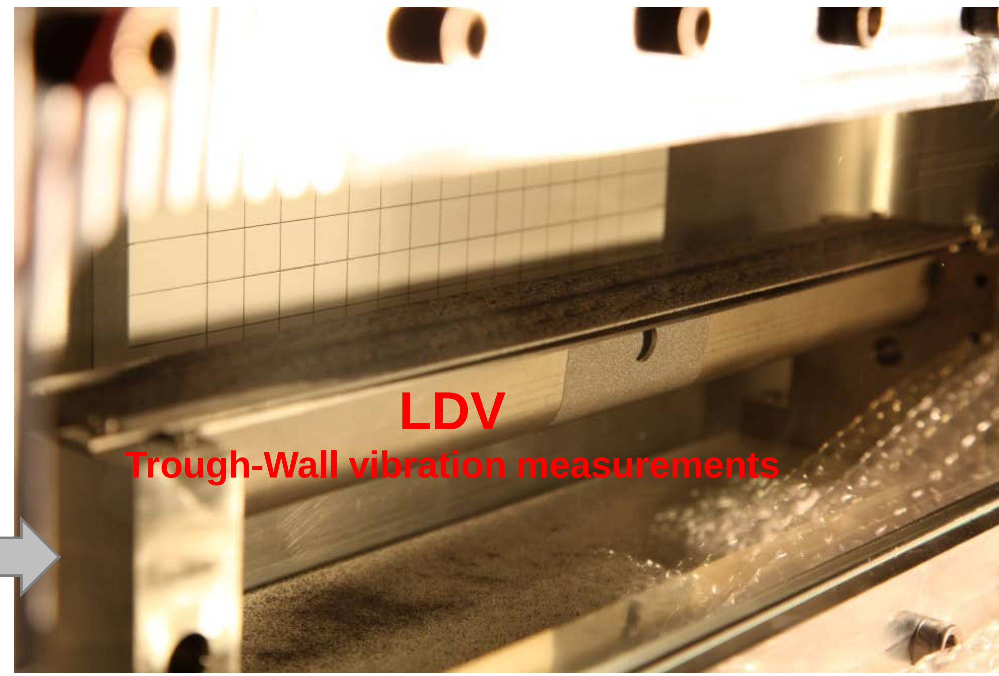

Trough photographed after the experiment.
Note: powder disruption

Science & Technology Facilities Council
Rutherford Appleton Laboratory

Interim Conclusions of HiRadMat experiment

- Fluidised powder jets generated by pulsed beams in sub-100 μm tungsten powder in helium environment
  - Eruption threshold of c.1.75 e11 ppp, σ = 1.17 mm
  - CFD model simulating a gas expansion eruption mechanism predicts threshold of c. 1 e12 ppp, σ = 2 mm
  - This discrepancy may be due to powder size distribution not modelled in CFX, but not understood yet
- But: powder jet velocities more than an order of magnitude less than those in mercury jet (MERIT experiment)
  - ~40x less than for mercury jet (with B=0)
  - ~10x less than for mercury jet (with B=10T)
- LDV data indicates container wall vibrations generated by secondary heating (as expected) and not by powder interaction with wall
- The driving force of the disruption is the gas expansion due to beam energy deposition. The movement of the grains are subject to the drag force of the container's gas atmosphere
- **Future experiment scheduled to:**
  - **separate effects in helium and vacuum environments**
  - **study effects of different grain sizes**

The very low measured maximum speed of the grains is a very encouraging indication for a future target system implementation !

Radiation damage "Here be dragons"

Subject of radiation damage intentionally left out from this talk.

Identified as "leading cross-cutting target facility challenge".

Good progress (experimental results; modelling).

Instead of a conclusion

Experiment Interesting new proposal: FETS-HIPSTER (Front End Test Stand – High Intensity Proton Source for Testing Effects of Radiation): 3 MeV protons; deep (~30 microns), near-uniform radiation damage to moderate levels within reasonable timescales (up to ~100 dpa per annum); Cheaper and shorter realisation time than proposed future irradiation facilities such as FAFNIR and IFMIF

Theory/modelling/cross sections see next talk